Thermodynamic and Kinetic Studies on Carbon−Cobalt Bond Homolysis by Ribonucleoside Triphosphate Reductase: The Importance of Entropy in Catalysis[†]

Stuart S. Licht,[‡] Christopher C. Lawrence,[‡] and JoAnne Stubbe*[,‡,§]

Departments of Chemistry and Biology, Massachusetts Institute of Technology, Cambridge, Massachusetts 02139

Received August 5, 1998; Revised Manuscript Received November 13, 1998

ABSTRACT: In the catalytic mechanism of nucleotide reduction, ribonucleoside triphosphate reductase (RTPR) from *Lactobacillus leichmannii* catalyzes the homolytic cleavage of the carbon−cobalt bond of adenosylcobalamin (AdoCbl) at a rate $\sim 10^{11}$-fold faster than the uncatalyzed reaction. Model systems have suggested hypotheses for the thermodynamic basis of this reaction, but relevant measurements of the enzymatic reaction have been lacking. To address this question in a system for which the microscopic rate constants can be measured as a function of temperature, we examined the RTPR-catalyzed exchange reaction. RTPR, in the presence of allosteric effector dGTP and in the absence of substrate, catalyzes carbon−cobalt bond homolysis and formation of a thiyl radical from an active-site cysteine in a concerted fashion [Licht, S., Booker, S., Stubbe, J. (1999) *Biochemistry 38*, 1221−1233]. Both the kinetics of cob(II)alamin formation and the amounts of cob(II)alamin formed have been studied as a function of AdoCbl concentration and temperature. Analysis of these data has allowed calculation of a ΔH of 20 kcal/mol, a ΔS of 70 cal mol^{-1} K^{-1}, a $\Delta H^{\ddagger}$ of 46 kcal/mol, and a $\Delta S^{\ddagger}$ of 96 cal mol^{-1} K^{-1} for carbon−cobalt bond homolysis/thiyl radical formation. The results further show that the enzyme perturbs the equilibrium between the reactant (AdoCbl-bound) state and the product (cob(II)alamin/5′-deoxyadenosine (5′-dA)/thiyl radical state, making them approximately equal in energy. The thermodynamic perturbation, in addition to transition-state stabilization, is required for the large rate acceleration observed. Entropic, rather than enthalpic, factors make the largest contribution in both cases.

One of the central mechanistic questions in the biochemistry of adenosylcobalamin (AdoCbl)[1] is how enzymes activate the carbon−cobalt bond of the coenzyme for homolytic bond cleavage. Studies from the Halpern and Finke laboratories determined that the homolytic bond dissociation energy of the carbon−cobalt bond is ∼30 kcal/mol in aqueous solution (*2*, *3*) and that the rate constant for this process is 10^{-9} s^{-1} at 25 °C (*4*). Carbon−cobalt bond homolysis has been shown to be an intermediate step in the mechanisms of enzymes that catalyze unusual carbon skeleton rearrangements (*5*) and in the mechanism of the enzyme that catalyzes ribonucleotide reduction (*6*). The turnover numbers of these enzymes vary from 2 to 300 s^{-1}, meaning that the enzymes must accelerate this process by a factor of at least 10^{10}−10^{12}. The mechanism of this rate acceleration for the AdoCbl-dependent ribonucleoside triphosphate reductase (RTPR) from *Lactobacillus leichmannii* is addressed in this paper.

RTPR catalyzes the conversion of nucleoside triphosphates to deoxynucleoside triphosphates. In the course of nucleotide reduction, a pair of cysteines at the active site is oxidized to a disulfide, making rereduction of the enzyme by an external reducing system necessary. During catalysis, the carbon−cobalt bond of AdoCbl is homolyzed to generate cob(II)alamin with an apparent first-order rate constant of >200 s^{-1} when a reducing system consisting of *Escherichia coli* thioredoxin (TR), *E. coli* thioredoxin reductase (TRR), and NADPH is used (S. Licht and J. Stubbe, unpublished results). Thus, RTPR accelerates this process by a factor of $\sim 1 \times 10^{11}$, which corresponds to a transition-state stabilization of ∼15 kcal/mol.

Many hypotheses have been advanced to explain the large rate enhancements of carbon−cobalt bond cleavage by enzymes (*7*, *8*). One hypothesis, based on structural and mechanistic studies of model organocobalt compounds (*9*−*13*), proposes that these enzymes induce a conformational change in the relatively flexible corrin ring, causing it to flex upward, applying a steric strain to the axial adenosyl moiety. Catalysis would thus result from the decrease in the carbon−cobalt bond dissociation energy of AdoCbl. The three-dimensional structure of AdoCbl in comparison with cob(II)alamin supports the hypothesis that homolysis is associated with upward flexing of the corrin ring (*14*). A second hypothesis proposes that the trans axial dimethylbenzimidazole ligand to cobalt is the key to catalysis. Model studies have shown that a weaker donor ligand causes the carbon−cobalt bond to become longer and the bond dis-

[†] This research was supported by grants from the National Institutes of Health to J.S. (GM 29595). S.L. was a Howard Hughes Medical Institute Predoctoral Fellow.

* Corresponding author.
[‡] Department of Chemistry.
[§] Department of Biology.

[1] Abbreviations: 5′-dA, 5′-deoxyadenosine; SF, stopped-flow; RTPR, ribonucleoside triphosphate reductase; AdoCbl, adenosylcobalamin; TR, thioredoxin; TRR, thioredoxin reductase; NADPH, β-nicotinamide adenine dinucleotide phosphate reduced form; dGTP, 2′-deoxyguanosine-5′-triphosphate; DTNB, dithionitrobenzoic acid; ES•, thiyl radical; E_a, activation energy.

10.1021/bi981886a CCC: $18.00
Published on Web 12/31/1998

sociation energy to decrease (*15*−*17*). In contrast, FT-Raman (*18*) and resonance Raman (*19*) studies have shown that, for alkylcobalamins, carbon−cobalt bond stretching frequencies do not depend on the trans axial ligand. Thus the role of the axial ligand is more complex than simply modulation of the carbon−cobalt bond strength. Whether the enzyme could thus accelerate this reaction by constraining the cobalt−nitrogen distance to be long or by protonating the imidazole to make it a weaker donating ligand is open to question.

Transition-state stabilization may provide an additional mechanism to accelerate carbon−cobalt bond homolysis. However, the fact that the activation energy for this process in solution (∼35 kcal/mol) (*4*) is not much greater than the bond dissociation energy suggests that selective stabilization of the transition state alone will not be able to provide the approximately 15 kcal/mol of stabilization required, because the transition state is only several kilocalories per mol higher in energy than the product (*2, 3*).

Finally, in both the enzymatic and model systems, entropic effects must be considered as a source of catalytic power. In the enzymatic case, solvent release from the enzyme or an increase in degrees of freedom of the cofactor and/or the enzyme could accompany progression along the reaction coordinate for carbon−cobalt bond homolysis.

To distinguish among these hypotheses, we can derive the relevant thermodynamic parameters from the temperature dependence of the microscopic rate constant for carbon−cobalt bond homolysis. The pre-steady-state kinetic analysis of carbon−cobalt bond homolysis in the presence of substrate is very complex, and work on deriving microscopic rate constants from the observed kinetics is still in progress. However, as described in the accompanying manuscript, RTPR catalyzes exchange of ^{3}H from [5′-^{3}H]-AdoCbl in the absence of substrate, requiring only a deoxynucleotide allosteric effector. Cob(II)alamin is an intermediate in this reaction as well, and, as our previous studies have revealed (*20, 21*), this reaction is an excellent model for the early stages of the nucleotide reduction process itself, since both reactions involve cofactor-mediated formation of cob(II)-alamin, 5′-deoxyadenosine (5′-dA), and an enzyme-based thiyl radical (ES$^\bullet$). An understanding of this simple model system has now allowed us to study the concentration and temperature dependence of the observed kinetics of RTPR-catalyzed carbon−cobalt bond homolysis and to derive microscopic rate constants and thermodynamic parameters associated with this process. These results suggest that catalysis is largely entropic in nature.

MATERIALS AND METHODS

General Methods. Nucleotides, nucleosides, and NADPH were obtained from Sigma. RTPR (specific activity of 1.4 μmol of ATP reduced min^{-1} mg^{-1}), TR (specific activity of 300−700 μmol of dithionitrobenzoic acid (DTNB) reduced min^{-1} mg^{-1}) and TRR (specific activity of 3000−7000 μmol min^{-1} mg^{-1}) were isolated as previously described (*22*−*24*). UV−vis spectroscopy was performed on a Cary 3 or Hewlett-Packard 8452A spectrophotometer. Centricon-30 microconcentrators were obtained from Millipore. All operations involving AdoCbl were carried out under dim light or red light.

Stopped-flow (SF) studies were carried out using an Applied Photophysics DX.17MV stopped-flow spectrophotometer. Anaerobic conditions were not employed, as rates and amounts of cob(II)alamin formation were observed to be unaffected by the presence of atmospheric oxygen at times <1 s after mixing.

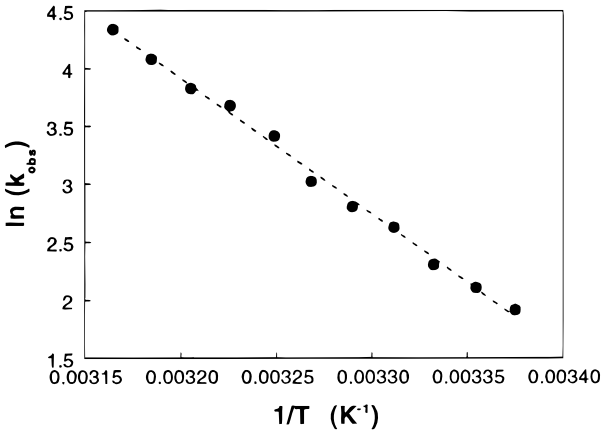

FIGURE 1: Temperature dependence of k_{obs}: $[RTPR]_0 = 20$ μM, $[AdoCbl]_0 = 100$ μM. Similar plots were obtained for all concentrations of RTPR and AdoCbl used. A linear least-squares fit was used to determine the slope and intercept of this plot, which were used to calculate the best-fit k_{obs} for any given temperature under these conditions. Analogous plots were generated for each set of conditions.

Concentrations of RTPR were measured spectrophotometrically ($\epsilon_{280} = 101\,000$ M^{-1} cm^{-1}) (*25*). Formation of cob(II)alamin was monitored using the decrease in absorption at 525 nm. For the conversion of AdoCbl to cob(II)alamin, $\Delta\epsilon = 4800$ M^{-1} cm^{-1} (*6*). Linear and nonlinear least-squares fits were carried out using either the Applied Photophysics system software or Kaleidagraph.

Stopped-Flow Studies on the Exchange Reaction: Dependence of Rates and Amounts of Cob(II)alamin Formation on [AdoCbl] and on Temperature. RTPR (6−80 μM), 20 μM TR, 1 μM TRR, 2 mM NADPH, and 1 mM dGTP in 200 mM sodium dimethylglutarate, pH 7.3, were mixed with an equal volume of the same reaction buffer containing variable amounts of AdoCbl (20 μM−1 mM) and 1 mM dGTP. For each set of concentrations, experiments were carried out at temperatures ranging from 25 to 40 °C. Traces were fit to a single or double exponential using the Applied Photophysics software. Double-exponential fits were required for [AdoCbl] ≥ 200 μM when the temperature was ≥ 37 °C.

The temperature was determined using the temperature detector in the SF spectrophotometer; this typically deviated from the bath temperature by ∼0.5 °C. When the temperature was changed, the system was allowed to equilibrate for at least 10 min before kinetic traces were recorded. The order of the temperature changes had no effect on the rate constants or amplitudes of the kinetic traces.

Derivation of Activation Parameters from the Temperature Dependence of k_{obs} as a Function of [AdoCbl]. The observed rate constants, k_{obs}, for cob(II)alamin formation were plotted as a function of temperature, 25−40 °C, in the form of an Arrhenius plot (ln(k_{obs}) vs 1/T, Figure 1). These plots were generated for every [AdoCbl] tested. The linear functions that gave the best fits to these plots were used to interpolate k_{obs} values for a variety of temperatures, and the k_{obs} values so obtained were plotted as a function of [AdoCbl] for each temperature (Figure 2). This procedure has the effect of

Scheme 1

$$\text{E-SH} + \text{AdoCbl} \underset{}{\overset{K_1}{\rightleftharpoons}} \text{E-SH} \cdot \text{AdoCbl} \underset{k_{-2}}{\overset{k_{+2}}{\rightleftharpoons}} \text{E-S}^{\bullet} \cdot \text{cob(II)alamin} \cdot \text{5'-dA}$$

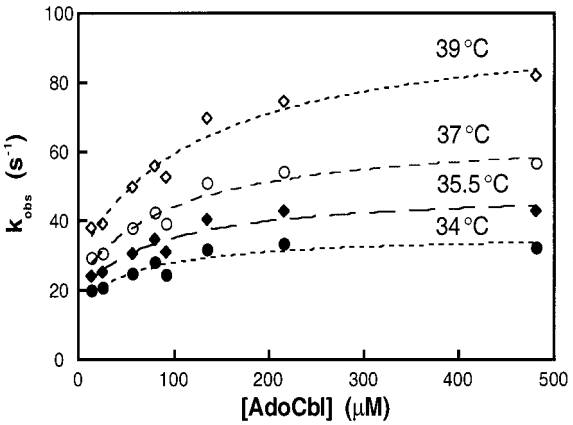

FIGURE 2: [AdoCbl] dependence of k_{obs} as a function of temperature. Equation 1 provided K_1, k_{+2}, and k_{-2} at each temperature, using k_{obs} interpolated from plots similar to that shown in Figure 1 and different [AdoCbl]s.

averaging out random errors in the determination of k_{obs} as a function of temperature, since the best-fit value, rather than k_{obs} as determined at each temperature, is used. For the k_{obs} values measured above 34 °C, precise fits to the concentration dependence of the calculated k_{obs} could be obtained (Figure 2). Below 34 °C, this was not possible given the scatter in the data. By using k_{obs} from these plots, K_1, k_{+2}, and k_{-2} (Scheme 1) were derived using eq 1 (*26*), originally derived for the small perturbations from equilibrium observed with relaxation methods, but also appropriate for large perturbations when one reactant is in large excess over the other. Because the linked equilibria under consideration contain a bimolecular step, AdoCbl binding, the rate constant for the approach to equilibrium depends on the concentration of the cofactor. Equation 1 describes this concentration dependence quantitatively. On a qualitative level, eq 1 indicates that the contribution of k_{+2} to k_{obs} is proportional to the saturation of enzyme with cofactor and that under saturating conditions $k_{obs} = k_{+2} + k_{-2}$.

$$k_{obs} = k_{+2}\left(\frac{K_1[\text{AdoCbl}]_0}{K_1[\text{AdoCbl}]_0 + 1}\right) + k_{-2} \qquad (1)$$

k_{obs} is obtained as described above. The $[\text{AdoCbl}]_0$ is the starting concentration of AdoCbl, as under all experimental conditions, its concentration is in 4−10-fold excess over [RTPR]. Global fitting of the SF traces (see Supporting Information) to the simple concerted model (Scheme 1) gives values of k_{+2}, k_{-2}, and K_1 similar to those obtained with eq 1, suggesting that the approximations employed in deriving eq 1 do not introduce large errors.

Once K_1, k_{+2}, and k_{-2} are known at each temperature, individual activation parameters can be derived using the Eyring theory and an Eyring plot [($\ln(k/T)$ vs $1/T$] from the general equation

$$\ln(k/T) = \ln(k_B/h) - \Delta H^{\ddagger}/RT + \Delta S^{\ddagger}/R \qquad (2)$$

where k is the rate constant (s^{-1}), R is the universal gas constant, T is the temperature (in K), k_B is the Boltzmann constant, and h is Planck's constant, $\Delta H^{\ddagger}$ is the enthalpy of activation (assumed to be equal to the activation energy, E_a), and $\Delta S^{\ddagger}$ is the entropy of activation (*27*). Individual activation parameters were derived for the temperature range of 34−40 °C, due to the scatter in the [AdoCbl] dependence data at lower temperatures, as described above.

Derivation of Thermodynamic Parameters from the Temperature Dependence of [Cob(II)alamin]∞/[RTPR]0 as a Function of [AdoCbl]. An analogous approach was used to derive thermodynamic parameters from the variation of steady-state amounts of cob(II)alamin formed as a function of temperature and [AdoCbl]. The fraction of enzyme in the form of ES•/cob(II)alamin/5′-dA in the steady state, ν, was plotted as a function of temperature in the form of a van't Hoff plot ($\ln \nu$ vs $1/T$). The linear functions that give the best fits to these plots were used to obtain values for ν at a variety of temperatures. These values for ν were then plotted as a function of [AdoCbl] for each temperature (Figure 5). K_1 and K_2 (k_2/k_{-2}) were derived from these plots using eq 3 (derived as described in (*28*)).

$$\nu = \frac{K_2K_1[\text{AdoCbl}]_0}{1 + K_1[\text{AdoCbl}]_0 + K_2K_1[\text{AdoCbl}]_0} \qquad (3)$$

The use of this equation allows the determination of both the binding constant for AdoCbl (K_1) and the equilibrium constant for carbon−cobalt bond homolysis/ES• formation (K_2). This equation takes into account all three states of RTPR (Scheme 1), and can compensate for the problem that the [AdoCbl] bound to RTPR cannot be distinguished spectroscopically from that free in solution. As was the case for k_{obs}, the most precise fits to the concentration dependence of the calculated ν were obtained with data at temperatures above 34 °C. Thermodynamic parameters were thus also derived for a narrow temperature range (34−40 °C), although the data used to derive these parameters were taken from the plot of $\ln \nu$ vs $1/T$ over the temperature range 25−40 °C. To obtain enthalpies (ΔH) and entropies (ΔS) of reaction, the temperature dependence of the equilibrium constants K_1 and K_2 was analyzed according to the van't Hoff equation:

$$\ln(K) = \frac{-\Delta H}{RT} + \frac{\Delta S}{R} \qquad (4)$$

For analysis of thermodynamic parameters associated with K_1, a standard state of 1 M was used.

Determination of Equilibrium Constant for Carbon−Cobalt Bond Homolysis/ES• Formation. RTPR (1 mM), 60 μM TR, 1.5 μM TRR, 2 mM NADPH, and 1 mM EDTA in 200 mM sodium dimethylglutarate, pH 7.3, were mixed in a septum-sealed Eppendorf tube which was purged with argon (blown over the solution) for 20 min while stirring at 0 °C. This mixture was transferred via gastight syringe to a septum-sealed, argon-purged cuvette at 37 °C, and the UV−vis spectrum was recorded. This background spectrum was essential because, at the high protein and NADPH concentrations used, these components had significant absorption

(∼0.1 absorbance units total) above 400 nm, where the spectra of the cobalamins absorb. Degassed AdoCbl was then added (final concentration of 70 μM), and the UV−vis spectrum was recorded. Finally, dGTP was added to a final concentration of 1 mM, and the spectrum was again recorded. The entire process took 5 min. Prolonged incubation was avoided as irreversible formation of cob(II)alamin has been observed (*29*).

RESULTS

Effect of [AdoCbl] on Kinetics of Cob(II)alamin Formation. Our studies (*30*) suggest that RTPR in the reduced form in the presence of allosteric effector dGTP catalyzes formation of cob(II)alamin, 5′-dA, and ES$^{\bullet}$ from reaction of AdoCbl with C408 of RTPR in a concerted fashion (Scheme 1). AdoCbl binds to RTPR rapidly and reversibly, indicated by K_1. The rate constants k_2 and k_{-2} correspond to the reversible concerted homolysis reaction. K_2 is the equilibrium constant for this process (k_2/k_{-2}). To derive values for k_2 and k_{-2} so that their temperature dependence can be evaluated, we determined the effect of [AdoCbl] on the kinetics of cob(II)alamin formation experimentally.

Previous studies (*1*) suggested that the K_d for AdoCbl is large (70−200 μM), providing a framework for the initial design of our experiments. An actual K_d has not thus far been measured due to to the ability of RTPR to catalyze the slow breakdown of AdoCbl (*29*).[2] When [AdoCbl] is large compared to [RTPR], k_{obs} for cob(II)alamin formation is given by eq 1 (see Materials and Methods).[3] Cob(II)alamin formation was analyzed by SF UV−vis spectroscopy over a range of [AdoCbl]s varying from 10 to 500 μM. In each experiment, AdoCbl was initially present in 4−10-fold excess over RTPR (3−40 μM). At each set of concentrations, measurements were made from 25 to 40 °C and k_{obs} was obtained by exponential fits to SF UV−vis traces. At temperatures ≥37 °C and above 200 μM AdoCbl, cob(II)alamin formation was biphasic, with the second kinetic phase at 37 °C, having a rate constant of ∼5 s^{-1} and an amplitude of 15−20% of the first phase. In these cases only the rate constants of the faster, larger amplitude phase are used. As discussed in detail in Supporting Information, the second phase may represent an alternate conformation for the RTPR−AdoCbl complex that does not accelerate carbon−cobalt bond homolysis as efficiently (Scheme S1).

Nonlinear least-squares fits of k_{obs} to eq 1 give k_2, k_{-2}, and K_1. At 37 °C, for example, $k_2 = 55 \pm 7$ s^{-1}, $k_{-2} = 27 \pm 2$ s^{-1}, and $K_1 = 5100 \pm 1700$ M^{-1}. The equilibrium constant for the second step, K_2, at this temperature is calculated to be 2.0 ± 0.3. The error in K_1 is large because it is not possible to determine rates with a saturating concentration of AdoCbl; above ∼500 μM, the A_{525} of AdoCbl is too high for accurate measurement in the available cells. With the experimental conditions used, binding of AdoCbl in any alternate binding mode associated with a small amount of cob(II)alamin formation will have a minimal effect on the rate constant for the faster phase of cob(II)alamin formation, as only a small fraction of AdoCbl will be bound in the alternate mode compared to the amount free in solution.

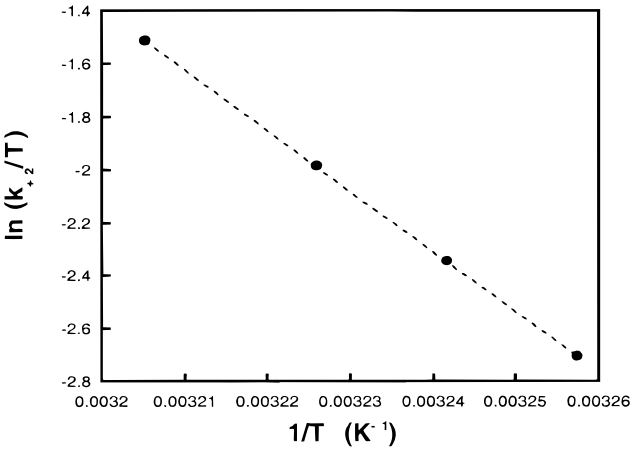

FIGURE 3: Eyring plot for k_{+2}. Data from Figure 2 and eq 2 provide k_{+2} over a range of temperatures. A linear least-squares fit is shown, with the slope of $\Delta H^{\ddagger}_2/R$ and the intercept equal to $\Delta S^{\ddagger}_2/R$.

While the magnitude of K_1 is not precisely defined, the data suggest that K_d for AdoCbl is 200 ± 67 μM . This is in accord with the observed K_m for AdoCbl (60 ± 9 μM) (*30*) in the exchange reaction and our inability to measure AdoCbl binding using a variety of standard methods (*20*). It also suggests that, although the reaction studied here almost certainly mimics early events in nucleotide reduction, it is unlikely to be physiologically important, as the physiological concentrations of AdoCbl are not sufficiently high to allow much binding in the absence of substrate (*31*, *32*).

Temperature Dependence of Kinetics of Cob(II)alamin Formation. For two coupled reactions such as the two steps in Scheme 1, k_{obs} contains contributions from both the forward and reverse steps of each reaction. To obtain activation parameters for each step, we measured the temperature dependence of k_{obs} as a function of [AdoCbl]. Given that k_2 and k_{-2} can be determined at each temperature, an Eyring plot (ln(k/T) vs 1/T) allows determination of the thermodynamic parameters (eq 2).

Each [AdoCbl] examined gave a plot analogous to Figure 1. Because the fits of the data to lines are good ($R^2 \sim 0.99$), these plots allow accurate prediction of k_{obs} at any temperature within the range measured. Plotting the calculated k_{obs} values as a function of [AdoCbl] (Figure 2) and the use of eq 1 allow calculation of the microscopic rate constants K_1, k_{+2}, and k_{-2} at different temperatures.

An Eyring plot (Figure 3, eq 2) allows the calculation of an activation enthalpy ($\Delta H^{\ddagger}_{+2}$) of 46 ± 7 kcal/mol and an activation entropy ($\Delta S^{\ddagger}_{+2}$) of 96 ± 12 cal mol^{-1} K^{-1} for the homolysis step, k_2. The large value for $\Delta H^{\ddagger}_{+2}$ suggests that the enzyme does not function to strain or weaken the carbon−cobalt bond in the ground-state enzyme−AdoCbl complex. The large value for $\Delta S^{\ddagger}_{+2}$ suggests that an increase in entropy in the transition state provides much of the transition-state stabilization in catalysis. The free energy of

[2] The one value for K_d that has been reported was measured under conditions where carbon−cobalt bond homolysis is known to occur (*1*).

[3] Because the K_d for AdoCbl is high, this approximation ([AdoCbl] ≈ [AdoCbl]$_0$) holds even at ratios of [AdoCbl]/[RTPR] less than 10, as long as [AdoCbl] ≪ K_d. Under these conditions, most of the AdoCbl remains unbound at equilibrium, so its concentration is approximately constant over the course of the reaction. Analysis of the amounts of cob(II)alamin observed using eq 2 (see Materials and Methods) indicated that, under all of the conditions used, bound forms of AdoCbl (the Michaelis complex and cob(II)alamin + 5′-dA) represented ≤15% of the total [AdoCbl], verifying the validity of approximating [AdoCbl] as [AdoCbl]$_0$.

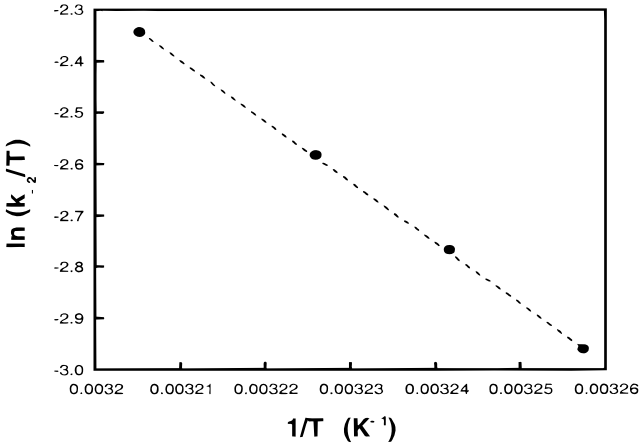

FIGURE 4: Eyring plot for k_{-2}. Data from Figure 2 and eq 2 provide k_{-2} over a range of temperatures. A linear least-squares fit is shown, with the slope of $\Delta H^{\ddagger}_{-2}/R$ and the intercept equal to $\Delta S^{\ddagger}_{-2}/R$.

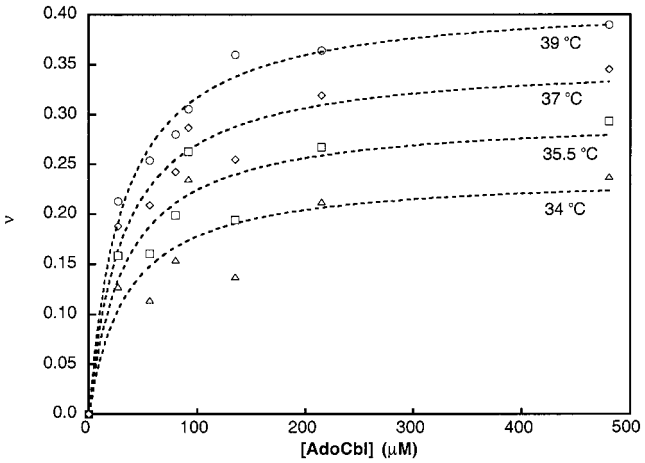

FIGURE 5: [AdoCbl] dependence of ν (the fraction of total enzyme in ES•/5′−dA/cob(II)alamin form) as a function of temperature. The data are fit to eq 3.

activation ($\Delta G^{\ddagger}_{+2}$) can be calculated from the relation $\Delta G^{\ddagger} = \Delta H^{\ddagger} - T\Delta S^{\ddagger}$ to be 16 ± 3 kcal/mol at 37 °C.

A similar analysis of the temperature dependence of k_{-2} (Figure 4) allows calculation of $\Delta H^{\ddagger}_{-2}$ of 26 ± 3 kcal/mol and $\Delta S^{\ddagger}_{-2}$ of 25 ± 12 cal mol^{-1} K^{-1}. The calculated $\Delta G^{\ddagger}_{-2}$ is 18 ± 5 kcal/mol.

The activation parameters for k_{+2} and k_{-2} allow determination of ΔH ($\Delta H^{\ddagger}_{+2} - \Delta H^{\ddagger}_{-2}$) and ΔS ($\Delta S^{\ddagger}_{+2} - \Delta S^{\ddagger}_{-2}$) for step 2 (Scheme 1). ΔH is 20 ± 8 kcal/mol, and ΔS is 70 ± 17 cal mol^{-1} K^{-1}. The value of 20 ± 8 kcal/mol is approximately equal to the net enthalpy change expected from the bonds broken and formed during this reaction (carbon−cobalt bond broken, ∼+30 kcal/mol, S−H bond broken ∼+90 kcal/mol, C−H bond formed, ∼−100 kcal/mol) (*33*−*35*). The experimental error in this value is too large to rule out any role for strain in homolysis. The data suggest, however, that the carbon−cobalt bond strength of RTPR-bound AdoCbl is close to that of free AdoCbl (that is, the enzyme does not act to exert much strain on the carbon−cobalt bond in the RTPR−AdoCbl-bound state). The large entropy of reaction indicates that an increase of degrees of freedom in the solvent, the protein, and/or the cofactor accompanies carbon−cobalt bond homolysis.

In principle, the enthalpy and entropy of AdoCbl binding could be determined from the temperature dependence of K_1. However, the error in K_1 is too large (up to 150%) to obtain reliable values. K_1 is observed to decrease with temperature, consistent with binding being exothermic (data not shown).

Effect of [AdoCbl] on Amounts of Cob(II)alamin Formation. The SF experiments also show how the amount of cob(II)alamin formed depends on the [AdoCbl]. The amplitude of the absorbance change (ΔA_{525}) in these experiments gives the amount of cob(II)alamin formed at equilibrium. As described above, the data are well-fit to a single exponential. However, two exponentials are needed to fit the time course of the absorbance change at [AdoCbl] ≥200 μM and at temperatures >37 °C. The faster kinetic phase (80−85% of the total absorbance change) was used for analysis of the amplitudes, as it was used to obtain the observed rate constants.

For the concerted mechanism in Scheme 1, ν, defined as [E−S•−5′-dA−cob(II)alamin]/[RTPR]$_0$, is given by eq 3 when AdoCbl is in large excess over RTPR. The equilibrium constants derived by this method require a knowledge of the number of active sites per RTPR. We have used a number of 0.8 sites based on the number of dNTPs produced in our single-turnover experiments (*20*) and on equilibrium binding studies of allosteric effectors (*36*). At 37 °C, plotting ν against [AdoCbl]$_0$, and fitting to eq 3 gives a K_1 of 21 000 ± 5 000 M^{-1} and a K_2 of 0.65 ± 0.05 (Figure 5), corresponding to free energies of ∼−6 kcal/mol and ∼0.03 kcal/mol, respectively. While the value for the overall K_{eq} (K_1*K_2) are the same within experimental error as the value obtained from k_{obs}, the value for K_1 is significantly higher and K_2 is significantly lower. This observation might be explained by the existence of one or more alternate modes of binding for AdoCbl that either do not allow cob(II)alamin formation or favor binding of AdoCbl over carbon−cobalt bond homolysis (see Supporting Information for a detailed analysis of an alternative binding mode).

Temperature Dependence of Amounts of Cob(II)alamin Formation. The amplitude data (ν) from SF experiments provide an independent check on the values of ΔH and ΔS for step 2. Measurement of ν over a range of temperatures at each concentration of RTPR and AdoCbl used and its change as a function of temperature were plotted in the form of a van't Hoff plot (data not shown). For each concentration of RTPR and AdoCbl employed experimentally, the equations from linear least-squares fits to the data were used to calculate values for ν at different temperatures. These values were plotted to give the [AdoCbl] dependence of ν at a variety of temperatures (Figure 5). Using eq 3, the equilibrium constants K_1 and K_2 were then calculated as a function of temperature. As was the case for the data derived from k_{obs}, the errors in K_1 are too large to obtain a reliable estimate of thermodynamic parameters associated with binding. However, a van't Hoff plot of K_2 as a function of temperature (Figure 6, eq 4) allows the determination of $\Delta H_2 = 12 \pm 5$ kcal/mol, in agreement with the values predicted from analysis of k_{obs} to within about one standard deviation. ΔS_2 is calculated to be 40 ± 15 cal mol^{-1} K^{-1}, in agreement with the value obtained from the analysis of k_{obs} to within about one standard deviation. These values are lower than those derived from the analysis of k_{obs} and are attributed to different enthalpy and entropy changes associated with the

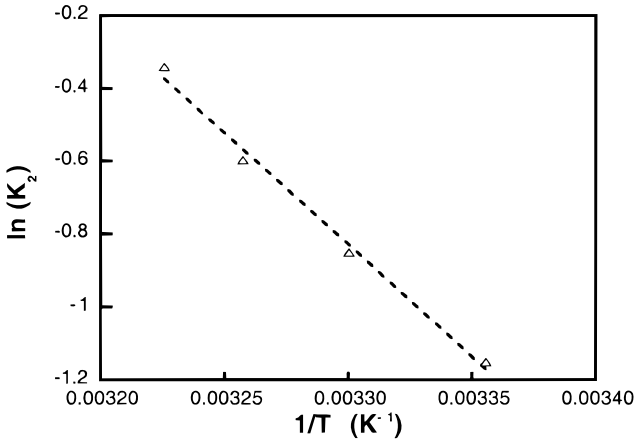

FIGURE 6: van't Hoff plot for K_2. The fits shown in Figure 5 provided values of K_2 over a range of temperatures. A linear least-squares fit is shown, with the slope equal to $\Delta H_2/R$ and the intercept equal to $\Delta S_2/R$.

alternate mode of binding ($K_{1'}$ in Scheme S1, Supporting Information). Further studies on binding of AdoCbl to the enzyme will be needed to resolve the question of an alternate binding mode and its thermodynamics. Nonetheless, both analysis of k_{obs} and analysis of ν are consistent with the entropic term, $T\Delta S_2$, contributing most of the difference between ΔG_2 and the corresponding free-energy change of nonenzymatic carbon−cobalt bond homolysis.

Determination of Cob(II)alamin Bound to RTPR when [RTPR]≫[AdoCbl]. If the initial binding equilibrium is saturated, the ratio of cob(II)alamin formed in the steady state to RTPR present should give K_2 directly (Scheme 1), providing another check on this value. Although measuring cob(II)alamin spectrophotometrically was not possible for [AdoCbl] > 500 μM, the availability of large amounts of RTPR allowed the binding equilibrium to be measured under conditions where $[RTPR]_0 \gg [AdoCbl]_0$, $[RTPR]_0 > K_d$. Under these conditions, the ratio of cob(II)alamin to AdoCbl should be approximately equal to K_2. This experiment was carried out by mixing (under anaerobic conditions) 1 mM RTPR with 70 μM AdoCbl in the presence of a reducing system and initiating carbon−cobalt bond cleavage by the addition of the allosteric effector dGTP. The SF UV−vis studies had indicated that the system would come to equilibrium in <1 s, so the change in the UV−vis spectrum was measured directly after mixing by hand.[4] We measured a ratio of cob(II)alamin to AdoCbl of 0.9 ± 0.1, in reasonable agreement with the values obtained above.

One contributor to systematic error in this experiment is the possibility that the binding of AdoCbl to RTPR (K_1) is not saturated. In this case, the ratio of cob(II)alamin to AdoCbl underestimates K_2. For example, if K_1 is 5100 M^{-1}, as estimated from the [AdoCbl] dependence of k_{obs} (eq 1), and the concentration of active sites is 0.8 mM rather than the 1 mM suggested by the A_{280} measurement, use of an equation equivalent to eq 3 (except that $[RTPR]_0$ replaces $[AdoCbl]_0$) shows that ∼10% of the AdoCbl would not be bound to RTPR. Thus, K_2 would be 1.1 ± 0.1, rather than 0.9 ± 0.1. The lower K_1 is, the greater the influence of this uncertainty will be.

Failure to saturate the binding associated with K_1 cannot account for the discrepancy between the K_2 calculated from this experiment and the K_2 calculated from the [AdoCbl] dependence of k_{obs} (2.0 ± 0.3). The existence of an alternate bound state (Scheme S1 Supporting Information) would lead to an underestimate of K_2 in this experiment, since some of the bound AdoCbl would not be in equilibrium with the ES•−cob(II)alamin−5′-dA form of the enzyme. The value calculated from this experiment should thus be considered an estimate of K_2.

Table 1: Summary of Rate and Equilibrium Constants Measured at 37 °C

	A[a]	B[b]	C[c]
K_1 (M^{-1})	5100 ± 1700	21 000 ± 5 000	
k_{+2} (s^{-1})	55 ± 7 s^{-1}		
k_{-2} (s^{-1})	27 ± 2 s^{-1}		
K_2	2.0 ± 0.3	0.65 ± 0.05	0.9 ± 0.1

[a] Measured by [AdoCbl] dependence of k_{obs} (Figure 2). [b] Measured by [AdoCbl] dependence of ν (Figure 5). [c] Measured by amount of cob(II)alamin formed when [RTPR] ≫ [AdoCbl].

Table 2: Thermodynamic Parameters

	A[a]	B[b]
ΔG_1 (kcal/mol)	∼−5	∼−6
$\Delta G^{‡}_{+2}$ (kcal/mol)	15.7 ± 0.1	
$\Delta G^{‡}_{-2}$ (kcal/mol)	16.1 ± 0.1	
ΔG_2 (kcal/mol)	−0.5 ± 0.1	∼−0.03
$\Delta H^{‡}_{+2}$ (kcal/mol)	46 ± 7	
$\Delta H^{‡}_{-2}$ (kcal/mol)	26 ± 3	
ΔH_2 (kcal/mol)	20 ± 8	12 ± 5
$\Delta S^{‡}_{+2}$ (cal/ mol^{-1} K^{-1})	96 ± 12	
$\Delta S^{‡}_{-2}$ (cal/ mol^{-1} K^{-1})	25 ± 12	
ΔS_2 (cal/ mol^{-1} K^{-1})	70 ± 17	40 ± 15

[a] Measured by [AdoCbl] dependence of k_{obs} (Figure 2). [b] Measured by [AdoCbl] dependence of ν (Figure 5).

The rate and equilibrium constants and thermodynamic parameters derived from analyses of rate constants and amplitudes of absorbance changes are summarized in Tables 1 and 2. As discussed subsequently, these thermodynamic parameters provide new insight into the mechanism by which RTPR catalyzes homolysis of the carbon−cobalt bond of AdoCbl and formation of a thiyl radical at C408.

DISCUSSION

RTPR catalyzes carbon−cobalt bond homolysis with a rate acceleration of ∼10^{11}-fold over the uncatalyzed reaction. The carbon−cobalt bond dissociation energy of ∼30 kcal/mol (*2*−*4*) for AdoCbl poses a fundamental obstacle for the large rate acceleration accomplished by RTPR. Since $T\Delta S$ is no more than ∼4 kcal/mol at 37 °C (*4*), ΔG for this reaction is about 26 kcal/mol. Stabilization of the transition state alone cannot decrease the activation free energy ($\Delta G^{‡}$) to less than ∼25 kcal/mol (Scheme 2a). However, the RTPR-catalyzed rate of carbon−cobalt bond homolysis corresponds to an activation free energy of ∼15 kcal/mol (Scheme 2b). The enzyme must therefore destabilize the reactant state (ESH−AdoCbl) and/or stabilize the product state (ES•−cob(II)-alamin−5′-dA) such that ΔG_2 is ≤15 kcal/mol (Scheme 2b).

[4] Slow (∼3 × 10^{-4} s^{-1}) irreversible formation of cob(II)alamin catalyzed by RTPR can be a major contributor to the uncertainty in experiments carried out by hand mixing. This irreversible reaction would artifactually increase the apparent value of K_2. Therefore, data obtained immediately after addition of dGTP to start the reaction was used for analysis.

Scheme 2

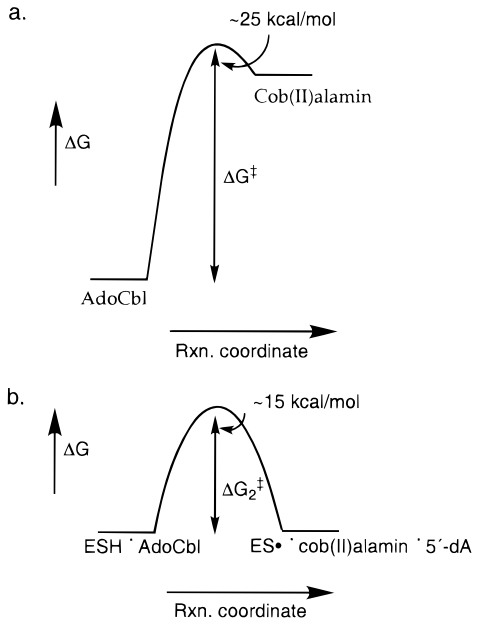

Only then can $\Delta G_2^{\ddagger}$ be $\leq$15 kcal/mol. An enzyme-mediated decrease in ΔH_2 and/or an enzyme-mediated increase in ΔS_2, through an increase in degrees of freedom of cofactor, protein, and/or solvent, could contribute to a decrease in ΔG_2.

The observation that the equilibrium constant for homolysis of the carbon−cobalt bond and ES• formation is on the order of one (2.0 ± 0.3) demonstrates that the thermodynamics of carbon−cobalt bond homolysis are in fact highly perturbed at the enzyme active site. The observed perturbation puts the AdoCbl-bound state at roughly the same free energy as the cob(II)alamin−5′-dA-bound ES• state ($\Delta G_2 \sim 0$). This observation is in accord with theoretical expectations for the relative free energies of reactive intermediates in enzyme mechanisms. For a concerted reaction, catalysis is predicted to be most efficient for reactions in which the intermediates are at equal energies, whether the reaction coordinate is analyzed using a Brønsted formalism (*37*) or a Marcus formalism (*38*).

To address the question of how RTPR solves the problem of efficient catalysis of a reaction that is highly endergonic in solution, we investigated the thermodynamics of carbon−cobalt bond homolysis on RTPR. In the absence of substrate, the kinetics are simple enough to determine microscopic rate constants for a concerted mechanism (Scheme 1). Measuring the rate and amount of cob(II)alamin formation as a function of temperature addresses two related questions. First, it provides information about how the enzyme controls the relative energies of the AdoCbl-bound state and the ES•−cob(II)alamin−5′-dA state, by allowing calculation of ΔH and ΔS. Second, it allows calculation of activation parameters ($\Delta H^{\ddagger}$ and $\Delta S^{\ddagger}$), thus defining the factors likely to be important in transition-state stabilization. In the case of RTPR, entropy appears to play an important role in establishing the thermodynamics and kinetics of carbon−cobalt bond homolysis.

Brown and Li have recently published a report of experiments similar to those carried out in this work. The primary differences in experimental methods were their use of dithiothreitol, rather than TR/TRR/NADPH, as the reductant and that their kinetic experiments were not carried out under pseudo-first-order conditions (*39*). In their work, biphasic Eyring plots for k_{+2} are reported, with the activation parameters derived at temperatures below 30 °C being similar to those reported here. Above 30 °C, their $\Delta H^{\ddagger}$ is 20 ± 1 kcal/mol and their $\Delta S^{\ddagger}$ is 13± 4 cal mol^{-1} K^{-1}, this latter value being significantly lower than the values reported here. Brown and Li suggest that the higher $\Delta H^{\ddagger}$ and $\Delta S^{\ddagger}$ they measure at low temperature (and, by implication, the values reported here over the entire temperature range) can be explained by a highly endothermic transition from an active enzyme conformation to a less-active enzyme conformation. The data from our experiments, however, are inconsistent with a kinetically observable step occurring before carbon−cobalt bond homolysis (*30*).

The experimental data (i.e., the temperature dependence of k_{obs} and the amount of cob(II)alamin formed) in Brown and Li's work is qualitatively similar to the data reported here. The differences between our results and theirs thus reflect differences in experimental design and consequently the differences in methods of analysis. We have designed our experiments to be carried out under pseudo-first-order conditions and have used eqs 1 and 3 for our analysis. Brown and Li's experiments were not in general carried out under pseudo-first-order conditions. The equations they used to analyze their data make approximations that are dependent on the magnitude of K_2. Equation 2 of Brown and Li is a special case of eq 3 used in this work. Their equation, derived in Supporting Information, requires the approximation that $K_2 \ll 1$. Furthermore, use of eq 4 in Brown and Li requires the approximation that $K_2 \gg 1$. However, our results, as well as those of Brown and Li, indicate that K_2 is approximately 1, suggesting that their use of these approximations is not valid. Finally, it should be noted that the specific activity of the RTPR used in their experiments is 20% of that of our RTPR and that the effects of the reductant on RTPR conformation are well-documented and may further contribute to the differences in reported activation parameters.

Entropy Drives Carbon−Cobalt Bond Cleavage/ES• Formation. Part of the large perturbation in the thermodynamics of carbon−cobalt bond cleavage can be explained by the enthalpically favorable coupling of this process to ES• and 5′-dA formation. ΔH_2 for this step is the sum of four enthalpy changes: that of the carbon−cobalt bond of AdoCbl bound to RTPR, that of the S−H bond of the catalytically required cysteine residue (C408), that of the C−H bond in 5′-dA, and that associated with conformational changes of RTPR. The measured ΔH_2 is ∼12−20 kcal/mol. The enthalpy for the analogous nonenzymatic set of reactions can be estimated to be 17−22 kcal/mol: ΔH_{C-Co}, 30−35 kcal/mol (*4*); ΔH_{RS-H}, 88 kcal/mol (*34*, *35*); and ΔH_{C-H}, 101 kcal/mol (*33*). The nonenzymatic value is within our error equivalent to that measured in the enzymatic reaction, consistent with the idea that binding of AdoCbl to RTPR does not result in a significant alteration of the carbon−cobalt bond dissociation energy. This result contrasts with expectations, based on extensive structural and mechanistic studies of model cobalamins and cobaloximes, that AdoCbl-dependent enzymes would perturb the thermodynamics of carbon−cobalt bond homolysis by weakening the carbon−cobalt bond through steric strain (*9*−*13*) and/or electronic effects (*15*−*17*).

The observed equalization of energies of AdoCbl and ES•−cob(II)alamin−5′-dA on RTPR and the similar values for ΔH for homolysis on and off the enzyme require that entropy makes an important contribution to this reaction. In fact, ΔS (40−70 cal mol^{-1} K^{-1}) associated with the enzymatic process differs significantly from the ΔS (14 cal mol^{-1} K^{-1}) (*4*) for carbon−cobalt bond homolysis in solution. Although entropy associated with the conformational mobility of the propionamide side chains of the corrin macrocycle (*39*, *40*) may make small contributions to ΔS, positive entropy changes of this magnitude in biological systems have usually been associated with changes in solvation.

Two examples of biological systems with measured ΔS values of 100 cal mol^{-1} K^{-1} are the polymerization of tobacco mosaic virus protein (*41*, *42*) and the interaction between the *trp* RNA-binding attenuation protein of *Bacillus subtilis* and *trp* leader RNA (*43*). In both cases the ΔH values for the reactions are unfavorable and the positive ΔS values are thought to be associated with release of H_2O. A third example is associated with allosteric transitions in hemoglobin. Ackers and co-workers have determined enthalpies and entropies for the conformational transitions associated with cooperative ligand (oxygen or cyanide) binding. They find a ΔH between the unliganded and fully liganded states of ∼30 kcal/mol and a ΔS of 80−90 cal mol^{-1} K^{-1} (*44*, *45*).

Using the above systems as models for RTPR, one proposal for the large ΔS is that a conformational change in the protein could switch the enzyme from a state in which the cofactor binding site is open to solvent to a state in which the cofactor binding site is desolvated and covered by another domain of the protein. While further studies are required to understand the basis for this large ΔS, its magnitude shows that this factor clearly plays an important role in the enzyme-mediated perturbation of the thermodynamics of carbon−cobalt bond homolysis required for catalysis.

$\Delta S^{\ddagger}$ Dominates Transition-State Stabilization for Carbon−Cobalt Bond Cleavage/ES• Formation. While the role of the enzyme in stabilizing intermediate species is important for catalysis, rate acceleration also depends on stabilization of the transition state of a reaction. Surprisingly, our studies revealed (Table 2) that $\Delta H_2^{\ddagger}$ for step 2 (Scheme 1) of 46 ± 7 kcal/mol is greater than $\Delta H^{\ddagger}$ of 30−35 kcal/mol measured in solution (*2*−*4*). This result suggests that RTPR does not weaken this bond in the AdoCbl-bound state. In addition, this result shows that an increase in enthalpically favorable enzyme−AdoCbl interactions on progressing to the transition state cannot account for the observed rate enhancement.

Two factors may account for the larger $\Delta H^{\ddagger}$ relative to that for AdoCbl. First, $\Delta H^{\ddagger}$ of nonenzymatic thiyl radical formation from a carbon-centered radical is ∼4 kcal/mol (*46*). The fact that RTPR exhibits kinetic isotope effects with [5′-$^2H_2$]−AdoCbl and D_2O suggests that a similar contribution is likely to be significant in the enzymatic system as well (*30*).

Second, the enthalpy of "cage escape", the diffusion of radicals out of the solvent cage, may have an analogue in enzymatic systems, which could contribute to the observed increase in $\Delta H_2^{\ddagger}$ (*47*). In model systems, cage effects have been shown to influence both $\Delta S^{\ddagger}$ and $\Delta H^{\ddagger}$ (*48*). These effects increase $\Delta H^{\ddagger}$ because they involve repulsive interactions between the escaping radical and their surrounding solvent (*49*, *48*), and because the escaping radical can disrupt favorable solvent−solvent interactions such as hydrogen bonds and van der Waals interactions. The $\Delta H^{\ddagger}$ for carbon−cobalt bond homolysis in ethylene glycol is ∼4.5 kcal/mol higher than the values measured in water, consistent with the relative viscosities of the solvents (*4*). Finke and co-workers have hypothesized that the AdoCbl binding sites of enzymes may serve as extremely efficient radical cages, able to adopt a conformation in which cage escape is highly efficient, allowing abstraction of hydrogen from the substrate or a protein residue (*47*). The activation energy of the conformational change required for efficient cage escape could in the case of RTPR thus contribute to an increase in $\Delta H_2^{\ddagger}$.

In contrast to expectations, $\Delta S_2^{\ddagger}$, ∼96 cal mol^{-1} K^{-1}, is the key to the observed rate acceleration contributing about −30 kcal/mol to $\Delta G_2^{\ddagger}$ at 37 °C. Mechanistic studies on model and enzymatic systems suggest a variety of possible sources that could contribute to this large $\Delta S_2^{\ddagger}$.

Many of the same factors that might influence the entropy change of the overall reaction can also influence the activation entropy. Cage effects in metal−ligand bond homolysis have effects on observed $\Delta S^{\ddagger}$ similar to those that they have on observed $\Delta H^{\ddagger}$ (*48*). In the few systems for which $\Delta S^{\ddagger}$ has been measured, it is on the order of 5−10 cal mol^{-1} K^{-1} (*48*, *50*).

The entropy associated with the conformational mobility of the propionamide side chains may also contribute to $\Delta S^{\ddagger}$. Homolysis of neopentylcobalamin bound to haptocorrin is 4.3 cal mol^{-1} K^{-1} greater than in solution (*40*). If this effect is similar in RTPR, it cannot by itself account for a major percentage of the observed $\Delta S^{\ddagger}$.

Model studies of Halpern and co-workers have shown a direct correlation between increasing $\Delta S^{\ddagger}$ and increasing $\Delta H^{\ddagger}$ for carbon−cobalt bond homolysis in a large group of organocobalt compounds. This trend is ascribed to transition states that increasingly resemble the products, nonplanar cobalt (II) complexes that are expected to be less rigid than the starting complexes (*51*). However, even for the most endothermic reaction examined ($\Delta H^{\ddagger}$ = 35 kcal/mol), $\Delta S^{\ddagger}$ is only 27 cal mol^{-1} K^{-1}. This effect, again, cannot be uniquely responsible for the magnitude of $\Delta S_2^{\ddagger}$ observed with RTPR.

The largest contributor to $\Delta S_2^{\ddagger}$, in analogy with ΔS_2, is likely to be a release of bound water from hydrophobic regions or an increase in conformational entropy of the protein. If the RTPR−AdoCbl complex leaves hydrophobic regions of the enzyme and/or AdoCbl partially solvated, a conformational change might allow contacts between these regions, leading to their desolvation. While the magnitude of the entropy change is large, the amount of hydrophobic surface that would have to be desolvated is likely to represent a reasonably small fraction of the total surface area. A free-energy change of 25−50 cal is associated with desolvation of 1 Å^2 of hydrophobic surface of a protein (*52*, *53*). A transition-state stabilization of 30 kcal/mol (to compensate for a $\Delta H^{\ddagger}$ of ∼45 kcal/mol) would thus require desolvation of ∼1000 Å^2 of hydrophobic surface. A conformational change causing a change in solvent accessible area of this magnitude would be reasonable for an 82 kDa protein such as RTPR. Hexokinase (MW = 100 kDa) undergoes a

conformational change on substrate binding that results in the release of ~65 water molecules (*54*), which, if each water molecule is assumed to take up 9−10 Å of surface (*55*), would correspond to desolvation of ~600 Å^2 of protein surface. Whether desolvation of hydrophobic regions of RTPR is a viable explanation for the observed activation parameters awaits the determination of three-dimensional structures of RTPR in apo- and cob(II)alamin−5′-dA-complexed forms.

SUMMARY

Steady-state and pre-steady-state analysis of carbon−cobalt bond homolysis/ES$^\bullet$ formation catalyzed by RTPR in the presence of dGTP has allowed the determination of rate constants using a minimal mechanism for the exchange reaction. Analysis of the temperature dependence of the rates and amounts of cob(II)alamin has allowed the determination of the thermodynamic parameters for this process. This analysis shows that entropic effects play an unexpected and large role in catalysis. Differential solvation of the ground state and the transition state is suggested as a possible source of the observed entropic effects.

SUPPORTING INFORMATION AVAILABLE

Global analysis of the kinetic data (Figure S1) using a concerted mechanism (Scheme 1 and Scheme S1), derivation of a special case of eq 3 when $K_2 \ll 1$, and analysis of the kinetic data in terms of a model with an alternate binding mode for AdoCbl (9 pages). Ordering information is given on any current masthead page.

REFERENCES

1. Singh, D., Tamao, Y., and Blakley, R. L. (1977) *Adv. Enzyme Regul. 15*, 81−101.
2. Finke, R. G., and Hay, B. P. (1984) *Inorg. Chem. 23*, 3041−3043.
3. Halpern, J., Kim, S.-H., and Leung, T. W. (1984) *J. Am. Chem. Soc. 106*, 8317−8319.
4. Hay, B. P., and Finke, R. G. (1988) *Polyhedron 7*, 1469−1481.
5. Dolphin, D. (1982) *B12*, John Wiley & Sons, New York.
6. Tamao, Y., and Blakley, R. L. (1973) *Biochemistry 12*, 24−34.
7. Halpern, J. (1985) *Science 227*, 869−875.
8. Banerjee, R. (1997) *Chem. Biol. 4*, 175−186.
9. Schrauzer, G. N., and Grate, J. H. (1979) *J. Am. Chem. Soc. 101*, 4601−4611.
10. Chemaly, S. M., and Pratt, J. M. (1980) *J. Chem. Soc., Dalton Trans.*, 2274−2281.
11. Randaccio, L., Bresciani-Pahor, N., Toscano, P. J., and Marzilli, L. G. (1981) *J. Am. Chem. Soc. 103*, 6347.
12. Geno, M. K., and Halpern, J. (1987) *J. Am. Chem. Soc. 109*, 1238−1240.
13. Kräutler, B., Konrat, R., Stupperich, E., Gerald, F., Gruber, K., and Kratky, C. (1994) *Inorg. Chem. 33*, 4128−4139.
14. Kratky, K., Färber, G., Gruber, K., Wilson, K., Dauter, Z., Nolting, H.-F., Konrat, R., and Kräutler, B. (1995) *J. Am. Chem. Soc. 117*, 4654−4670.
15. Ng, F. T. T., and Rempel, G. L. (1982) *J. Am. Chem. Soc. 104*, 621−623.
16. Marzilli, L. G., Summers, M. F., Bresciani-Pahor, N., Zangrando, E., Charland, J.-P., and Randaccio, L. (1985) *J. Am. Chem. Soc. 107*, 6880−6888.
17. De Ridder, D. J. A., Zangrando, E., and Bürgi, H.-B. (1996) *J. Mol. Struct. 374*, 63−83.
18. Puckett, J. M. J., Mitchell, M. B., Hirota, S., and Marzilli, L. G. (1996) *Inorg. Chem. 35*, 4656−4662.
19. Dong, S., Padmakumar, R., Banerjee, R., and Spiro, T. G. (1996) *J. Am. Chem. Soc. 118*, 9182−9183.
20. Booker, S., Licht, S., Broderick, J., and Stubbe, J. (1994) *Biochemistry 33*, 12679−12685.
21. Licht, S., Gerfen, G. J., and Stubbe, J. (1996) *Science 271*, 477−481.
22. Lunn, C. A., Kathju, S., Wallace, C., Kushner, S., and Pigiet, V. (1984) *J. Biol. Chem. 259*, 10469−10474.
23. Russel, M., and Model, P. (1985) *J. Bacteriol. 163*, 238−242.
24. Booker, S., and Stubbe, J. (1993) *Proc. Natl. Acad. Sci. U.S.A. 90*, 8352−8356.
25. Blakley, R. L. (1978) *Methods Enzymol. 51*, 246−259.
26. Bernasconi, C. (1976) *Relaxation Kinetics*, Academic Press, New York.
27. Tinoco, I., Sauer, K., and Wang, J. C. (1985) *Physical Chemistry*, Prentice-Hall, Englewood Cliffs, NJ.
28. Eisenberg, D., and Crothers, D. (1979) *Physical Chemistry with Applications to the Life Sciences*, Benjamin/Cummings, Menlo Park, CA.
29. Yamada, R., Tamao, Y., and Blakley, R. L. (1971) *Biochemistry 10*, 3959−3968.
30. Licht, S., and Stubbe, J. (1999) *Biochemistry 38*, 1221−1233.
31. Davis, R. L., Layton, L. L., and Chow, B. F. (1952) *Proc. Soc. Exp. Biol. Med. 79*, 273−276.
32. Kashket, S., Kaufman, J. T., and Beck, W. S. (1962) *Biochim. Biophys. Acta 64*, 447−457.
33. Benson, S. W. (1978) *Chem. Rev. 78*, 23−35.
34. McMillen, D. F., and Golden, D. M. (1982) *Annu. Rev. Phys. Chem. 33*, 493−532.
35. Griller, D., and Martinho Simoes, J. A. (1990) *Sulfur-Centered Reactive Intermediates in Chemistry and Biology* (Chatgilialoglu, C., and Asmus, K.-D., Eds.) Plenum Press, New York.
36. Chen, A. K., Bhan, A., Hopper, S., Abrams, R., and Franzen, J. S. (1974) *Biochemistry 13*, 654−661.
37. Albery, W. J., and Knowles, J. R. (1976) *Biochemistry 15*, 5631−5640.
38. Gerlt, J. A., and Gassman, P. G. (1993) *J. Am. Chem. Soc. 115*, 11552−11568.
39. Brown, K. L., Cheng, S., and Marques, H. M. (1995) *Inorg. Chem. 34*, 3038−3049.
40. Brown, K. L., Evans, D. R., Cheng, S., and Jacobsen, D. W. (1996) *Inorg. Chem. 35*, 217−222.
41. Banerjee, K., and Lauffer, M. (1966) *Biochemistry 5*, 1957−1963.
42. Lauffer, M. (1975) *Entropy-Driven Processes in Biology: Polymerization of Tobacco Mosaic Virus Protein and Similar Reactions*, Springer, Berlin, Germany.
43. Baumann, C., Otridge, J., and Gollnick, P. (1996) *J. Biol. Chem. 271*, 12269−12274.
44. Mills, F. C., and Ackers, G. K. (1979) *Proc. Natl. Acad. Sci. U.S.A. 76*, 273−277.
45. Huang, Y., and Ackers, G. K. (1995) *Biochemistry 34*, 6316−6327.
46. Zavitsas, A. A., and Chagilialoglu, C. (1995) *J. Am. Chem. Soc. 117*, 10645−10654.
47. Garr, C. D., and Finke, R. G. (1993) *Inorg. Chem. 32*, 4414−4421.
48. Koenig, T. W., Hay, B. P., and Finke, R. G. (1988) *Polyhedron 7*, 1499−1516.
49. Franck, J., and Rabinowitch, E. (1934) *Trans. Faraday Soc. 32*, 120.
50. Herkes, F. E., Friedman, J., and Bartlett, P. D. (1969) *Int. J. Chem. Kinet. 1*, 193−207.
51. Halpern, J. (1988) *Bull. Chem. Soc. Jpn. 61*, 13−15.
52. Chothia, C., and Janin, J. (1975) *Nature 256*, 705.
53. Williams, D. H. (1991) *Aldrichimica Acta 24*, 71−80.
54. Rand, R. P., Fuller, N. L., Butko, P., Francis, G., and Nicholls, P. (1993) *Biochemistry 32*, 5925−5929.
55. Colombo, M. F., Rau, D. C., and Parsegian, V. A. (1992) *Science 256*, 655−659.

BI981886A